Feasibility issues in static output-feedback controller design with application to structural vibration control

F. Palacios-Quiñonero[a], J. Rubió-Massegú[a], J. M. Rossell[a], H. R. Karimi[b,*]

[a]*Dept. of Applied Mathematics III, Universitat Politècnica de Catalunya (UPC), 08242-Manresa, Spain*
[b]*Dept. of Engineering, Faculty of Engineering and Science, University of Agder (UiA), N-4898 Grimstad, Norway*

Abstract

Recent results in output-feedback controller design make possible an efficient computation of static output-feedback controllers by solving a single-step LMI optimization problem. This new design strategy is based on a simple transformation of variables, and it has been applied in the field of vibration control of large structures with positive results. There are, however, some feasibility problems that can compromise the effectiveness and applicability of the new approach. In this paper, we present some relevant properties of the variable transformations that allow devising an effective procedure to deal with these feasibility issues. The proposed procedure is applied in designing a static velocity-feedback H_∞ controller for the seismic protection of a five-story building with excellent results.

1. Introduction

Limited access to the state variables information is a common problem in most practical control applications. In this context, static output-feedback controllers are a very interesting option [1, 2]. To synthesize static output-feedback controllers, a variety of multi-step numerical algorithms have been proposed, as those based on random search [3], or those consisting in iterative procedures [4–6]. Typically, these methods require solving complex matrix equations or linear matrix inequality (LMI) optimization problems at each step. To avoid the high computational cost associated to the multi-step methods, some single-step strategies have also been proposed [7–10]. These single-step methods are based on a proper transformation of the state variables and formulate the static output-feedback controller design in terms of a single LMI optimization problem. Nevertheless, this second line of solution presents the drawback of being highly problem-dependent, in the sense that most controller designs require a complete derivation of the associated LMI optimization problem.

The latest trends in vibration control of large structures consider distributed control systems formed by a large number of sensors and actuation devices, together with a wide and sophisticated

*Corresponding author

Email addresses: francisco.palacios@upc.edu (F. Palacios-Quiñonero), josep.rubio@upc.edu (J. Rubió-Massegú), josep.maria.rossell@upc.edu (J. M. Rossell), hamid.r.karimi@uia.no (H. R. Karimi)

communications network [11, 12]. This kind of control systems present particularly challenging design characteristics, such as high dimensionality, severe information constraints and fast real-time operation requirements [13–16] . Clearly, static output-feedback strategies can play a major role in this scenario. However, it also becomes apparent that effective numerical algorithms are of critical importance for the practical applicability of this approach to large scale control problems.

Following the ideas presented by Zečević and Šiljak [17–19], a new control design strategy for seismic protection of large structures has been proposed in [20–22]. The new approach allows computing static output-feedback controllers by solving a single-step LMI optimization problem, which can be easily derived from the associated state-feedback LMI formulation through simple transformations of the LMI variables. In all these works, however, the LMI optimization problems associated to the output-feedback controller designs are initially reported to be infeasible by the MATLAB LMI optimization tools [23], and a slightly perturbed state matrix has to be used to overcome this computational difficulty. Recently, more general transformations of the LMI variables have been proposed in [24]. In the present paper, an effective line of solution to the aforementioned feasibility issues is obtained by taking advantage of the additional design flexibility provided by these generalized LMI-variable transformations.

The paper is organized as follows: In Section 2, the fundamental elements of the new output-feedback controller design strategy are provided. In Section 3, an accurate study of some relevant properties of the generalized LMI-variable transformations is presented, and a two-step design procedure is devised to deal with the feasibility issues. In Section 4, the effectiveness of the proposed two-step procedure is demonstrated by designing a static velocity-feedback H_∞ controller for the seismic protection of a five-story building. Finally, some conclusions and future research directions are presented in Section 5.

2. Theoretical background

Let us consider a control problem with state vector $x(t) \in \mathbb{R}^n$ and control vector $u(t) \in \mathbb{R}^m$. A wide variety of advanced state-feedback control designs can be formulated as an LMI optimization problem of the form

$$P_s : \begin{cases} \text{Minimize } h(\eta) \\ \text{subject to } X > 0,\ F(X,Y,\eta) < 0, \end{cases} \tag{1}$$

where $X \in \mathbb{R}^{n\times n}$ is a symmetric positive-definite matrix, $Y \in \mathbb{R}^{m\times n}$ is a general matrix, $\eta \in \mathbb{R}^p$ is a vector that collects the free entries not contained in X and Y, h is a real linear function, and F is an affine map that makes the matrix inequality $F(X,Y,\eta) < 0$ an LMI. In this case, an optimal state-feedback controller $u(t) = G_s x(t)$ is usually obtained by computing an optimal triplet $\left(\tilde{X}_s, \tilde{Y}_s, \tilde{\eta}_s\right)$ for the LMI problem in Eq. (1), and by setting $G_s = \tilde{Y}_s \tilde{X}_s^{-1}$.

Let us now assume that the information available for feedback purposes consists in a vector of observed outputs $y(t) \in \mathbb{R}^q$ with $q < n$, which can be expressed as $y(t) = C_y x(t)$ for a given observed-output matrix $C_y \in \mathbb{R}^{q\times n}$ with full row-rank. To design a static output-feedback controller $u(t) = K y(t)$, we can consider the state-feedback controller $u(t) = G_K x(t)$ with $G_K = K C_y$ and

solve the optimization problem

$$P_{of}: \begin{cases} \text{Minimize } h(\eta) \\ \text{subject to } X > 0,\ F(X,Y,\eta) < 0, (X,Y) \in \mathscr{M}, \end{cases} \tag{2}$$

where $\mathscr{M}$ is the set of all pairs of matrices (X,Y) for which there exists a matrix $K \in \mathbb{R}^{m\times q}$ that satisfies $YX^{-1} = KC_y$. A suitable LMI formulation for the output-feedback optimization problem P_{of} can be obtained by using the following change of variables:

$$X = QX_QQ^T + RX_RR^T, \quad Y = Y_RR^T, \tag{3}$$

where $X_Q \in \mathbb{R}^{(n-q)\times(n-q)}$ and $X_R \in \mathbb{R}^{q\times q}$ are symmetric positive-definite matrices, $Y_R \in \mathbb{R}^{m\times q}$ is a general matrix, $Q \in \mathbb{R}^{n\times(n-q)}$ is a matrix whose columns are a basis of $\ker(C_y)$, and $R \in \mathbb{R}^{n\times q}$ is a matrix of the form

$$R = C_y^\dagger + QL, \tag{4}$$

where $L \in \mathbb{R}^{(n-q)\times q}$ is a given matrix, and $C_y^\dagger = C_y^T(C_yC_y^T)^{-1}$ is the *Moore-Penrose pseudoinverse* of C_y. According to the results presented in [24], if the LMI optimization problem

$$P_c: \begin{cases} \text{Minimize } h(\eta) \\ \text{subject to } X_Q > 0,\ X_R > 0,\ F(QX_QQ^T + RX_RR^T, Y_RR^T, \eta) < 0 \end{cases} \tag{5}$$

attains an optimal solution for the quartet $\left(\tilde{X}_Q, \tilde{X}_R, \tilde{Y}_R, \tilde{\eta}_c\right)$ then, for the triplet $\left(\tilde{X}_c, \tilde{Y}_c, \tilde{\eta}_c\right)$ with $\tilde{X}_c = Q\tilde{X}_QQ^T + R\tilde{X}_RR^T$ and $\tilde{Y}_c = \tilde{Y}_RR^T$, the optimization problem P_{of} given in Eq. (2) achieves a suboptimal solution with $K = \tilde{Y}_R\tilde{X}_R^{-1}$. Note that the optimal value $\tilde{h}_{of}$ of the problem P_{of} must satisfy the inequality

$$\tilde{h}_s \le \tilde{h}_{of} \le \tilde{h}_c, \tag{6}$$

where $\tilde{h}_s$ and $\tilde{h}_c$ denote the optimal values of the problems P_s and P_c given in Eqs. (1) and (5), respectively.

The following lemmas will be used in obtaining the main results. The proofs of Lemma 1 and Lemma 2 can be found in [24]. The results presented in Lemma 3 are also used in [24], but without a detailed proof, which has been included here for completeness. In what follows, we assume that I and 0 denote, respectively, an identity matrix and a zero matrix of appropriate dimensions.

Lemma 1. *For a given $n \times n$ symmetric matrix $\hat{X}$, the following two conditions are equivalent:*

(i) $C_y\hat{X} = 0$,

(ii) $\hat{X} = QX_QQ^T$, *where X_Q is a symmetric matrix with dimensions $(n-q)\times(n-q)$.*

Moreover, if (i) and (ii) are satisfied, then (ii) holds with $X_Q = Q^\dagger\hat{X}(Q^\dagger)^T$, where $Q^\dagger$ is the Moore–Penrose pseudoinverse of Q, i.e. $Q^\dagger = (Q^TQ)^{-1}Q^T$.

Lemma 2. *The matrix inequality $QX_QQ^T + RX_RR^T > 0$ is equivalent to $X_Q > 0$ and $X_R > 0$.*

Lemma 3. *For a given $n \times q$ matrix R, the following two conditions are equivalent:*

(i) $C_yR = I$,

(ii) $R = C_y^\dagger + QL$, *where L is a matrix with dimensions $(n-q) \times q$.*

Moreover, when (i) and (ii) hold, $L = Q^\dagger R$ is the unique matrix that satisfies (ii).

PROOF. From $C_yC_y^\dagger = I$ and $C_yQ = 0$, we obtain $C_y(C_y^\dagger + QL) = I$ and, consequently, (ii) implies (i). Let us now assume that $C_yR = I$. In this case, we have $0 = C_yR - I = C_y(R - C_y^\dagger)$. As the columns of Q are a basis of $\ker(C_y)$, we can write $R - C_y^\dagger = QL$ for a suitable matrix L and, therefore, (i) implies (ii). Next, by observing that $Q^\dagger C_y^\dagger = 0$ and $Q^\dagger Q = I$, we get $Q^\dagger R = Q^\dagger C_y^\dagger + Q^\dagger QL = L$. Obviously, setting $R = C_y^\dagger + QL'$ and left-multiplying by $Q^\dagger$ leads to $L = Q^\dagger R = L'$.

3. Main results

The controller designs for seismic protection of large structures presented in [20–22] are carried out by using the LMI-variable transformations given in Eq. (3) with $R = C_y^\dagger$. This particular R-matrix can be obtained from the general expression in Eq. (4) by selecting a null matrix L. In all these works, however, the LMI optimization problem P_c in Eq. (5) is initially infeasible, and it is necessary to use a slightly perturbed state matrix in order to complete the controller design. In this section, we will see how the generalized form $R = C_y^\dagger + QL$ proposed in [24] introduces additional design flexibility that can be conveniently used to provide a more effective line of solution to these feasibility issues.

Let us consider the set $\mathscr{P}_n = \{X \in \mathbb{S}^{n\times n} : X > 0\}$ of all $n \times n$ symmetric positive-definite matrices. The following theorem states some relevant properties of the variable transformations defined in Eqs. (3) and (4).

Theorem 1. *For any $X \in \mathscr{P}_n$, there exists a unique matrix L such that $X = QX_QQ^T + RX_RR^T$ holds, with $R = C_y^\dagger + QL$, for suitable matrices $X_Q \in \mathscr{P}_{n-q}$ and $X_R \in \mathscr{P}_q$. Moreover, L can be written in the form $L = Q^\dagger XC_y^T \left(C_yXC_y^T\right)^{-1}$.*

PROOF. For a given $X \in \mathscr{P}_n$, let us consider the matrix $X_R = C_yXC_y^T$. As X is positive-definite and C_y has full row-rank, the matrix X_R is non-singular. Let us also consider the matrix

$$R = XC_y^T(C_yXC_y^T)^{-1}, \tag{7}$$

which satisfies

$$C_yR = C_yXC_y^T(C_yXC_y^T)^{-1} = I \tag{8}$$

and

$$X_RR^T = C_yXC_y^T(C_yXC_y^T)^{-1}C_yX = C_yX. \tag{9}$$

From (8) and (9), we obtain

$$C_y\left(X - RX_RR^T\right) = C_yX - X_RR^T = C_yX - C_yX = 0. \tag{10}$$

Next, by setting $\hat{X} = X - RX_RR^T$ in Lemma 1, we can affirm that there exists a symmetric matrix X_Q such that $X - RX_RR^T = QX_QQ^T$ and, consequently, X can be written in the form $X = QX_QQ^T + RX_RR^T$. Moreover, from Lemma 2, it follows that $X_Q > 0$ and $X_R > 0$. Considering Eq. (8) and Lemma 3, R can be written in the form $R = C_y^\dagger + QL$. Finally, from Lemma 3 and Eq. (7), the matrix L admits the expression $L = Q^\dagger R = Q^\dagger XC_y^T\left(C_yXC_y^T\right)^{-1}$. To prove the unicity of matrix L, let us suppose that X can be written in the form

$$X = Q\hat{X}_QQ^T + \hat{R}\hat{X}_R\hat{R}^T, \tag{11}$$

where $\hat{R}$ is a matrix that satisfies

$$\hat{R} = C_y^\dagger + Q\hat{L}, \tag{12}$$

for a suitable matrix $\hat{L} \in \mathbb{R}^{(n-q)\times q}$. From Eq. (12), we observe that $C_y\hat{R} = I$. Right-multiplying Eq. (11) by C_y^T and applying $Q^TC_y^T = 0$ and $\hat{R}^TC_y^T = I$, we obtain

$$XC_y^T = \hat{R}\hat{X}_R. \tag{13}$$

Left-multiplying Eq. (13) by C_y and using that $C_y\hat{R} = I$, we get $\hat{X}_R = C_yXC_y^T$. Hence, from Eq. (13), we can now derive

$$\hat{R} = XC_y^T\hat{X}_R^{-1} = XC_y^T(C_yXC_y^T)^{-1}, \tag{14}$$

which matches the expression in Eq. (7) and proves the unicity of matrix R. Finally, from Lemma 3, the unicity of matrix L also follows.

Now, for a given matrix $L \in \mathbb{R}^{(n-q)\times q}$, let us consider the set $\mathscr{V}_L$ of all matrices X that can be expressed in the form $X = QX_QQ^T + RX_RR^T$, where $X_Q \in \mathscr{P}_{n-q}$, $X_R \in \mathscr{P}_q$, and $R = C_y^\dagger + QL$ is the R-matrix corresponding to this particular choice of L. The following theorem shows that a classification of $\mathscr{P}_n$ is induced by the L matrices.

Theorem 2. *The family $\mathscr{V} = \{\mathscr{V}_L : L \in \mathbb{R}^{(n-q)\times q}\}$ defines a partition of $\mathscr{P}_n$.*

PROOF. According to Lemma 2, for any matrix L, we have $\mathscr{V}_L \subset \mathscr{P}_n$. Moreover, from Theorem 1, every matrix $X \in \mathscr{P}_n$ satisfies $X \in \mathscr{V}_{L_X}$ with

$$L_X = Q^\dagger XC_y^T\left(C_yXC_y^T\right)^{-1}. \tag{15}$$

Hence, we have $\mathscr{P}_n = \cup\mathscr{V}_L$. Also from Theorem 1, we get $\mathscr{V}_L \cap \mathscr{V}_{L'} = \varnothing$ for $L \neq L'$.

In the previous section, we have seen how the variable transformations defined in Eqs. (3) and (4) can make possible the effective computation of an output-feedback gain matrix in the form $K = \tilde{Y}_R \tilde{X}_R^{-1}$. However, this strategy also introduces additional constraints in the optimization problem. More precisely, after selecting a particular matrix L in Eq. (4), the problem P_c in Eq. (5) is equivalent to the following optimization problem:

$$P_L : \begin{cases} \text{Minimize } h(\eta) \\ \text{subject to } X \in \mathscr{V}_L,\ Y = Y_R R^T,\ F(X,Y,\eta) < 0, \end{cases} \tag{16}$$

which constrains the X matrices of the problem P_s to the variety $\mathscr{V}_L$, and the matrices $Y \in \mathbb{R}^{m\times n}$ to the form $Y = Y_R R^T$ with $Y_R \in \mathbb{R}^{m\times q}$. Consequently, it becomes now apparent that a suitable choice of the matrix L can have a significant influence on both the feasibility and the optimality level of the solutions provided by the associated output-feedback design strategy. The choice $R = C_y^\dagger$, used in [20–22], corresponds to the case $L = 0$. Obviously, this election can be fully justified on the basis of mathematical simplicity, however, it has nothing to do with the specific properties of the considered control problem.

Using the superior insight of the variable transformations provided by Theorems 1 and 2, a better design strategy can be defined by selecting the L-matrix corresponding to the optimal X-matrix obtained in the state-feedback problem P_s. Based on this choice, we can define the following two-step design procedure:

Step 1. Solve the state-feedback LMI optimization problem P_s given in Eq. (1).

Step 2. If the problem P_s in Step 1 attains an optimal value $\tilde{h}_s$ for the triplet $\left(\tilde{X}_s, \tilde{Y}_s, \tilde{\eta}_s\right)$, compute the matrix

$$\tilde{L} = Q^\dagger \tilde{X}_s C_y^T \left(C_y \tilde{X}_s C_y^T\right)^{-1}, \tag{17}$$

and solve the LMI optimization problem P_c given in Eq. (5) using the R-matrix

$$\tilde{R} = C_y^\dagger + Q\tilde{L}. \tag{18}$$

Remark 1. The proposed design procedure requires solving the state-feedback optimization problem P_s and, additionally, a second LMI optimization problem P_c with similar computational complexity. Hence, from a computational point of view, this approach can be potentially applied to any control design where the state-feedback LMI formulation attains positive results.

Remark 2. Step 1 in the design procedure can also be understood as an exploratory step. In fact, no further efforts should be invested in obtaining an output-feedback controller when no satisfactory solution is attained by the ideal full-state approach. Moreover, when Step 1 produces positive results, the state-feedback controller can be used as a natural reference to assess the performance of the output-feedback design.

Remark 3. For the choice $L = \tilde{L}$, the X matrices of the optimization problem $P_{\tilde{L}}$ in Eq. (16) are constrained to the variety $\mathcal{V}_{\tilde{L}}$ and, consequently, can take the optimal value $\tilde{X}_s$. In contrast, the additional constraint $Y = Y_R\tilde{R}^T$ can produce suboptimal results or even infeasibility. However, when the optimal state-feedback control matrix G_s can be factored in the form $G_s = KC_y$, we can write $\tilde{Y}_s\tilde{X}_s^{-1} = KC_y$ and obtain

$$\tilde{Y}_s = KC_y\tilde{X}_s = KC_y\left(QX_QQ^T + \tilde{R}X_R\tilde{R}^T\right) = KX_R\tilde{R}^T. \tag{19}$$

Hence, the matrix $\tilde{Y}_s$ can be factored in the form $\tilde{Y}_s = Y_R\tilde{R}^T$ with $Y_R = KX_R$ and, in this particular case, the problem $P_{\tilde{L}}$ is always feasible and attains the optimal value $\tilde{h}_s$.

Remark 4. Heuristic approaches are mainly sustained by successful practical applications. In this sense, it must be highlighted that the proposed design procedure is currently being applied to ongoing investigations in the field of vibration control of large structures with excellent results. An example of this line of work is provided in the next section.

4. Aplication to structural vibration control

In this section, the proposed two-step design procedure is applied to synthesize a velocity-feedback H_∞ controller for seismic protection of a five-story building. In Subsection 4.1, a suitable state-space model for the building is provided. Next, a state-feedback H_∞ controller is designed in Subsection 4.2. As indicated in Remark 2, this state-feedback controller will be used as a reference in the performance assessment. In Subsection 4.3, the velocity-feedback controller is computed by using the transformations of LMI variables defined by the L-matrix proposed in Eq. (17). Finally, in Subsection 4.4, numerical simulations of the building vibrational response are conducted to evaluate the effectiveness of the proposed velocity-feedback controller.

4.1. Building model

Let us consider the five-story building schematically depicted in Fig. 1. The building motion can be described by the second-order differential equation

$$M\ddot{q}(t) + C\dot{q}(t) + \bar{K}q(t) = T_u u(t) + T_w w(t), \tag{20}$$

where M and C denote the mass and damping matrices, respectively. The stiffness matrix has been represented by $\bar{K}$ to avoid confusion with the notation used for the output-feedback control gain matrix K. The vector of displacements relative to the ground is

$$q(t) = [q_1(t), q_2(t), q_3(t), q_4(t), q_5(t)]^T, \tag{21}$$

where $q_i(t)$, $1 \leq i \leq 5$, represents the lateral displacement of the ith story s_i with respect to the ground level s_0. We assume that an actuation device a_i has been implemented between the consecutive stories s_{i-1} and s_i, $1 \leq i \leq 5$. Each control device a_i exerts a control action $u_i(t)$, which produces a pair of structural opposite forces as indicated in Fig. 1(b). The vector of control actions is

$$u(t) = [u_1(t), u_2(t), u_3(t), u_4(t), u_5(t)]^T, \tag{22}$$

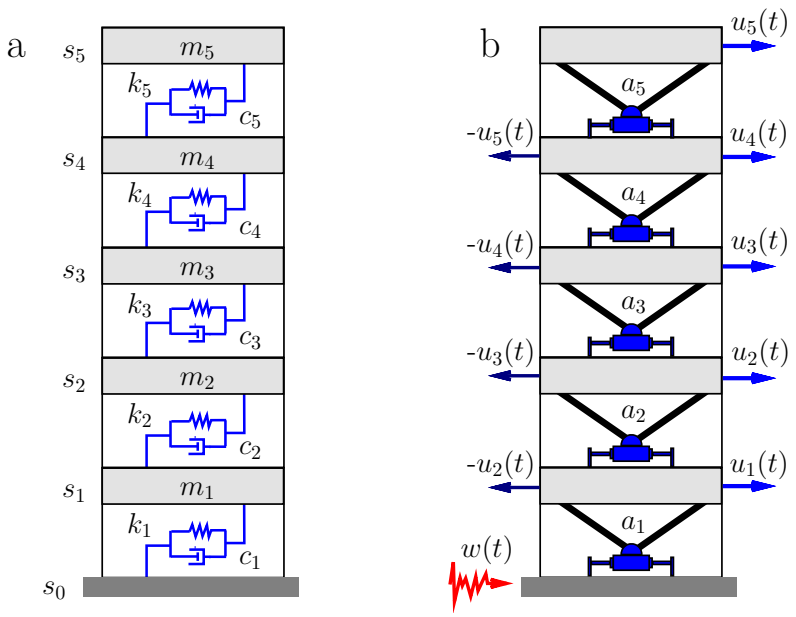

Figure 1: Five-story building: (a) mechanical model, (b) actuation scheme

T_u is the control location matrix, T_w is the excitation location matrix, and $w(t) \in \mathbb{R}$ denotes the seismic ground acceleration. In the controller designs and numerical simulations conducted in the present paper, the following particular values of the matrices M, C, $\bar{K}$, T_u, and T_w have been used:

$$M = 10^3 \times \begin{bmatrix} 215.2 & 0 & 0 & 0 & 0 \\ 0 & 209.2 & 0 & 0 & 0 \\ 0 & 0 & 207.0 & 0 & 0 \\ 0 & 0 & 0 & 204.8 & 0 \\ 0 & 0 & 0 & 0 & 266.1 \end{bmatrix}, \; C = 10^3 \times \begin{bmatrix} 650.4 & -231.1 & 0 & 0 & 0 \\ -231.1 & 548.9 & -202.5 & 0 & 0 \\ 0 & -202.5 & 498.6 & -182.0 & 0 \\ 0 & 0 & -182.0 & 466.8 & -171.8 \\ 0 & 0 & 0 & -171.8 & 318.5 \end{bmatrix}, \quad (23)$$

$$\bar{K} = 10^6 \times \begin{bmatrix} 260 & -113 & 0 & 0 & 0 \\ -113 & 212 & -99 & 0 & 0 \\ 0 & -99 & 188 & -89 & 0 \\ 0 & 0 & -89 & 173 & -84 \\ 0 & 0 & 0 & -84 & 84 \end{bmatrix}, \quad T_u = \begin{bmatrix} 1 & -1 & 0 & 0 & 0 \\ 0 & 1 & -1 & 0 & 0 \\ 0 & 0 & 1 & -1 & 0 \\ 0 & 0 & 0 & 1 & -1 \\ 0 & 0 & 0 & 0 & 1 \end{bmatrix}, \quad T_w = -M \begin{bmatrix} 1 \\ 1 \\ 1 \\ 1 \\ 1 \end{bmatrix}, \quad (24)$$

where masses are in kg, damping coefficients in Ns/m, and stiffness coefficients in N/m. The mass and stiffness values used in matrices M and $\bar{K}$ are similar to those presented in [25]; the damping matrix C has been computed as a Rayleigh damping matrix with a 5% damping ratio on the first and fifth modes [26]. Next, we consider the state vector

$$x(t) = \begin{bmatrix} q(t) \\ \dot{q}(t) \end{bmatrix}, \quad (25)$$

and derive a first-order state-space model

$$\dot{x}(t) = Ax(t) + Bu(t) + Ew(t), \quad (26)$$

with the system matrices

$$A = \begin{bmatrix} [0]_{5\times5} & I_5 \\ -M^{-1}\bar{K} & -M^{-1}C \end{bmatrix}, \quad B = \begin{bmatrix} [0]_{5\times5} \\ M^{-1}T_u \end{bmatrix}, \quad E = \begin{bmatrix} [0]_{5\times1} \\ -[1]_{5\times1} \end{bmatrix}, \tag{27}$$

where $[0]_{n\times m}$ represents a zero-matrix of the indicated dimensions, I_n is the identity matrix of order n, and $[1]_{n\times1}$ denotes a vector of dimension n with all its entries equal to 1. For the building matrices in Eq. (23) and Eq. (24), the following first-order system matrices result:

$$A = 10^3 \times \begin{bmatrix} 0 & 0 & 0 & 0 & 0 & 0.0010 & 0 & 0 & 0 & 0 \\ 0 & 0 & 0 & 0 & 0 & 0 & 0.0010 & 0 & 0 & 0 \\ 0 & 0 & 0 & 0 & 0 & 0 & 0 & 0.0010 & 0 & 0 \\ 0 & 0 & 0 & 0 & 0 & 0 & 0 & 0 & 0.0010 & 0 \\ 0 & 0 & 0 & 0 & 0 & 0 & 0 & 0 & 0 & 0.0010 \\ -1.2082 & 0.5251 & 0 & 0 & 0 & -0.0030 & 0.0011 & 0 & 0 & 0 \\ 0.5402 & -1.0134 & 0.4732 & 0 & 0 & 0.0011 & -0.0026 & 0.0010 & 0 & 0 \\ 0 & 0.4783 & -0.9082 & 0.4300 & 0 & 0 & 0.0010 & -0.0024 & 0.0009 & 0 \\ 0 & 0 & 0.4346 & -0.8447 & 0.4102 & 0 & 0 & 0.0009 & -0.0023 & 0.0008 \\ 0 & 0 & 0 & 0.3157 & -0.3157 & 0 & 0 & 0 & 0.0006 & -0.0012 \end{bmatrix} \tag{28}$$

$$B = 10^{-5} \times \begin{bmatrix} 0 & 0 & 0 & 0 & 0 \\ 0 & 0 & 0 & 0 & 0 \\ 0 & 0 & 0 & 0 & 0 \\ 0 & 0 & 0 & 0 & 0 \\ 0 & 0 & 0 & 0 & 0 \\ 0.4647 & -0.4647 & 0 & 0 & 0 \\ 0 & 0.4780 & -0.4780 & 0 & 0 \\ 0 & 0 & 0.4831 & -0.4831 & 0 \\ 0 & 0 & 0 & 0.4883 & -0.4883 \\ 0 & 0 & 0 & 0 & 0.3758 \end{bmatrix}, \qquad E = \begin{bmatrix} 0 \\ 0 \\ 0 \\ 0 \\ 0 \\ -1 \\ -1 \\ -1 \\ -1 \\ -1 \end{bmatrix}. \tag{29}$$

4.2. State-feedback H_∞ controller

Let us now consider the vector of interstory drifts

$$r(t) = [r_1(t), r_2(t), r_3(t), r_4(t), r_5(t)]^T, \tag{30}$$

where $r_i(t)$ denotes the relative displacement between the stories s_{i-1} and s_i, which can be computed as

$$\begin{cases} r_1(t) = q_1(t), \\ r_i(t) = q_i(t) - q_{i-1}(t), \quad \text{for} \quad 1 < i \leq 5. \end{cases} \tag{31}$$

Assuming that the objectives in the controller design are minimizing the interstory drift seismic response and the control efforts, we introduce the vector of controlled outputs

$$z(t) = C_z x(t) + D_z u(t), \tag{32}$$

where

$$C_z = \begin{bmatrix} C_r \\ [0]_{5\times10} \end{bmatrix}, \quad D_z = \alpha \begin{bmatrix} [0]_{5\times5} \\ I_5 \end{bmatrix}, \tag{33}$$

$$C_r = \begin{bmatrix} 1 & 0 & 0 & 0 & 0 & 0 & 0 & 0 & 0 & 0 \\ -1 & 1 & 0 & 0 & 0 & 0 & 0 & 0 & 0 & 0 \\ 0 & -1 & 1 & 0 & 0 & 0 & 0 & 0 & 0 & 0 \\ 0 & 0 & -1 & 1 & 0 & 0 & 0 & 0 & 0 & 0 \\ 0 & 0 & 0 & -1 & 1 & 0 & 0 & 0 & 0 & 0 \end{bmatrix}, \tag{34}$$

and $\alpha > 0$ is a suitable coefficient that trades-off the conflicting design objectives. The controlled output $z(t)$ satisfies

$$\{z(t)\}^T z(t) = \sum_{i=1}^{5} [r_i(t)]^2 + \alpha^2 \sum_{i=1}^{5} [u_i(t)]^2 \tag{35}$$

and it can be used to compute a state-feedback H_∞ controller

$$u(t) = G_s x(t). \tag{36}$$

The H_∞ control approach considers the largest energy gain from disturbance to controlled output

$$\gamma_G = \sup_{\|w\|_2 \neq 0} \frac{\|z\|_2}{\|w\|_2}, \tag{37}$$

where

$$z(t) = (C_z + D_z G)\, x(t) \tag{38}$$

is the closed-loop controlled output corresponding to the state-feedback controller $u(t) = Gx(t)$, $w(t)$ denotes the input disturbance, and $\|\cdot\|_2$ denotes the usual continuous 2-norm

$$\|f\|_2 = \left[\int_0^\infty \{f(t)\}^T f(t)\, dt \right]^{1/2}. \tag{39}$$

Broadly speaking, the controller design consists in obtaining a gain matrix G_s which produces an asymptotically stable closed-loop system

$$\dot{x}(t) = (A + BG_s)x(t) \tag{40}$$

and, simultaneously, attains an optimally small γ-value γ_{G_s}. It is well known that these objectives can be achieved by considering the LMI

$$\begin{bmatrix} AX + XA^T + BY + Y^T B^T + \eta EE^T & * \\ C_z X + D_z Y & -I \end{bmatrix} < 0, \tag{41}$$

where $*$ denotes the transpose element in the symmetric position, and solving the following LMI optimization problem:

$$P_s' : \begin{cases} \text{maximize } \eta \\ \text{subject to } X > 0,\ \eta > 0 \text{ and the LMI in Eq. (41).} \end{cases} \tag{42}$$

If an optimal value $\tilde{\eta}_s$ is attained for the matrices $\tilde{X}_s$ and $\tilde{Y}_s$, then the state-feedback gain matrix G_s can be written in the form $G_s = \tilde{Y}_s \tilde{X}_s^{-1}$, and the optimal γ-value can be computed as $\gamma_{G_s} = \tilde{\eta}_s^{-1/2}$. By solving the problem P_s' with the system matrices A, B, E given in Eqs. (28), (29), and the matrices C_z, D_z defined in Eqs. (33), (34), with $\alpha = 10^{-7.3}$, we obtain the following control gain matrix:

$$G_s = 10^6 \times \begin{bmatrix} -2.5816 & 1.1382 & -0.0094 & -0.0478 & -0.1782 & -0.2221 & -0.2817 & -0.3077 & -0.3359 & -0.4773 \\ 2.3696 & -3.4531 & 1.3062 & -0.1324 & -0.1595 & -0.0699 & -0.3251 & -0.3937 & -0.4238 & -0.5987 \\ 1.3637 & 2.5261 & -3.8190 & 1.0653 & -0.2166 & -0.0283 & -0.1034 & -0.4073 & -0.4608 & -0.6427 \\ 0.1086 & 1.2183 & 2.8212 & -3.9680 & 0.5651 & -0.0282 & -0.0583 & -0.1180 & -0.4505 & -0.6567 \\ 0.1494 & 0.0625 & 0.7261 & 3.1868 & -3.6136 & -0.0163 & -0.0326 & -0.0449 & -0.0841 & -0.6152 \end{bmatrix} \tag{43}$$

with an associated γ-value

$$\gamma_{G_s} = 0.06931. \tag{44}$$

Remark 5. The optimization problem P_s' defined in Eq. (42) can be written in the form given in Eq. (1) by setting $h(\eta) = -\eta$ and

$$F(X,Y,\eta) = \begin{bmatrix} AX + XA^T + BY + Y^T B^T + \eta EE^T & * & * \\ C_z X + D_z Y & -I & * \\ 0 & 0 & -\eta \end{bmatrix}. \tag{45}$$

4.3. Velocity-feedback H_∞ controller

Now, let us assume that the information available for feedback purposes consists in the inter-story velocities. We define the vector of observed outputs

$$y(t) = [\dot{r}_1(t), \dot{r}_2(t), \dot{r}_3(t), \dot{r}_4(t), \dot{r}_5(t)]^T, \tag{46}$$

which can be computed in the form $y(t) = C_y x(t)$, with

$$C_y = \begin{bmatrix} 0 & 0 & 0 & 0 & 0 & 1 & 0 & 0 & 0 & 0 \\ 0 & 0 & 0 & 0 & 0 & -1 & 1 & 0 & 0 & 0 \\ 0 & 0 & 0 & 0 & 0 & 0 & -1 & 1 & 0 & 0 \\ 0 & 0 & 0 & 0 & 0 & 0 & 0 & -1 & 1 & 0 \\ 0 & 0 & 0 & 0 & 0 & 0 & 0 & 0 & -1 & 1 \end{bmatrix}. \tag{47}$$

Following the design procedure proposed in Section 3, we can compute a velocity-feedback H_∞ controller $u(t) = K y(t)$ by considering the matrices

$$Q = \begin{bmatrix} 1 & 0 & 0 & 0 & 0 \\ 0 & 1 & 0 & 0 & 0 \\ 0 & 0 & 1 & 0 & 0 \\ 0 & 0 & 0 & 1 & 0 \\ 0 & 0 & 0 & 0 & 1 \\ 0 & 0 & 0 & 0 & 0 \\ 0 & 0 & 0 & 0 & 0 \\ 0 & 0 & 0 & 0 & 0 \\ 0 & 0 & 0 & 0 & 0 \\ 0 & 0 & 0 & 0 & 0 \end{bmatrix}, \qquad \tilde{R} = \begin{bmatrix} 0.0025 & 0.0048 & 0.0051 & 0.0041 & 0.0025 \\ 0.0015 & 0.0018 & 0.0047 & 0.0048 & 0.0030 \\ -0.0035 & -0.0029 & -0.0020 & 0.0015 & 0.0016 \\ -0.0099 & -0.0094 & -0.0082 & -0.0064 & -0.0018 \\ -0.0146 & -0.0141 & -0.0130 & -0.0112 & -0.0082 \\ 1.0000 & 0.0000 & 0.0000 & 0.0000 & 0.0000 \\ 1.0000 & 1.0000 & 0.0000 & 0.0000 & 0.0000 \\ 1.0000 & 1.0000 & 1.0000 & 0.0000 & 0.0000 \\ 1.0000 & 1.0000 & 1.0000 & 1.0000 & 0.0000 \\ 1.0000 & 1.0000 & 1.0000 & 1.0000 & 1.0000 \end{bmatrix}, \tag{48}$$

and the LMI

$$\begin{bmatrix} AQX_QQ^T + QX_QQ^TA^T + A\tilde{R}X_R\tilde{R}^T + \tilde{R}X_R\tilde{R}^TA^T + BY_R\tilde{R}^T + \tilde{R}Y_R^TB^T + \eta EE^T & * \\ C_zQX_QQ^T + C_z\tilde{R}X_R\tilde{R}^T + D_zY_R\tilde{R}^T & -I \end{bmatrix} < 0, \quad (49)$$

where A, B, E, C_z and D_z are the same matrices used in Subsection 4.2. In this case, the optimization problem

$$P_c' : \begin{cases} \text{maximize } \eta \\ \text{subject to } X_Q > 0,\, X_R > 0,\, \eta > 0, \text{ and the LMI in Eq. (49)}, \end{cases} \quad (50)$$

produces the following velocity-feedback gain matrix:

$$K = 10^6 \times \begin{bmatrix} -1.3700 & -1.3298 & -1.2209 & -1.0000 & -0.6328 \\ -1.5042 & -1.5523 & -1.5316 & -1.3101 & -0.8469 \\ -1.3135 & -1.4432 & -1.5455 & -1.3996 & -0.9271 \\ -0.9734 & -1.1248 & -1.3143 & -1.3037 & -0.9036 \\ -0.5589 & -0.6618 & -0.8148 & -0.8742 & -0.6798 \end{bmatrix}, \quad (51)$$

with an associated γ-value

$$\gamma_{G_K} \leq \tilde{\eta}_c^{-1/2} = 0.06934, \quad (52)$$

where $\tilde{\eta}_c$ denotes the optimal value obtained for the problem P_c' and $G_K = KC_y$.

Remark 6. No feasibility issues appear when solving the optimization problem P_c' with the LMI optimization tools of the MATLAB Robust Control Toolbox [23]. This fact contrasts with the situation encountered when using the transformations of LMI variables corresponding to the choice $L = 0$ in [20–22]. In this case, it was necessary to use a perturbed state matrix to overcome the initial unfeasibility of the LMI optimization problem.

Remark 7. As indicated in Eq. (52), the value $\tilde{\eta}_c^{-1/2}$ only provides an upper bound of the γ-value attained by the velocity-feedback controller $u(t) = Ky(t)$ (see [22]). This fact, however, is not relevant in the present problem since the values in Eqs. (44) and (52) indicate that the obtained velocity-feedback H_∞ controller is practically optimal.

4.4. Numerical results

For the five-story building presented in Subsection 4.1, let us consider the following control configurations: (i) *Uncontrolled*. No control system is implemented in the building. (ii) *State-feedback*. The building is equipped with the actuation system depicted in Fig.1(b), which is driven by the state-feedback H_∞ controller $u(t) = G_s x(t)$ defined by the gain matrix G_s given in Eq. (43). (iii) *Velocity-feedback*. The building is equipped with the same actuation system, but in this case the control actions are computed using the velocity-feedback controller $u(t) = Ky(t)$ defined by the gain matrix K given in Eq. (51).

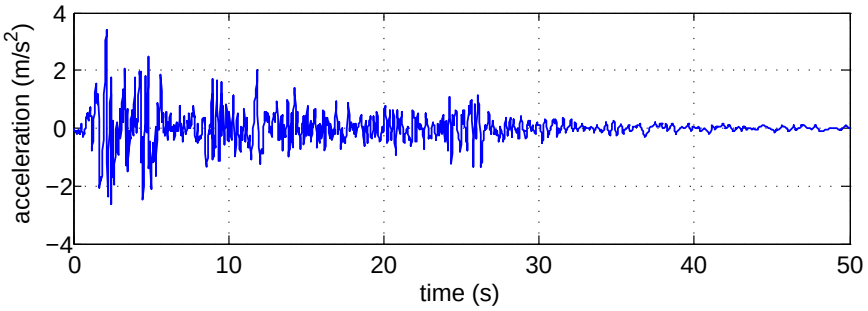

Figure 2: North–South 1940 El Centro seismic record.

For these three control configurations, numerical simulations of the building vibrational response have been conducted. Specifically, the full-scale North–South 1940 El Centro seismic record (see Fig. 2) has been taken as ground acceleration, and the corresponding vectors of interstory drifts $r(t)$ and control efforts $u(t)$ have been computed. To compare the performance of the different control configurations, we have considered the maximum absolute values:

$$\hat{r}_i = \max_{0\le t\le T} |r_i(t)|, \quad \hat{u}_i = \max_{0\le t\le T} |u_i(t)|, \quad 1 \le i \le 5, \tag{53}$$

where $[0,T]$ is simulation time interval.

The maximum absolute interstory drifts $\hat{r}_i$ are displayed in Fig. 3, where it can be clearly appreciated that a significant reduction in the interstory drifts peak-values are achieved by the state-feedback configuration (blue line with circles) and the velocity-feedback configuration (red line with asterisks), when compared with the uncontrolled configuration (black line with squares).

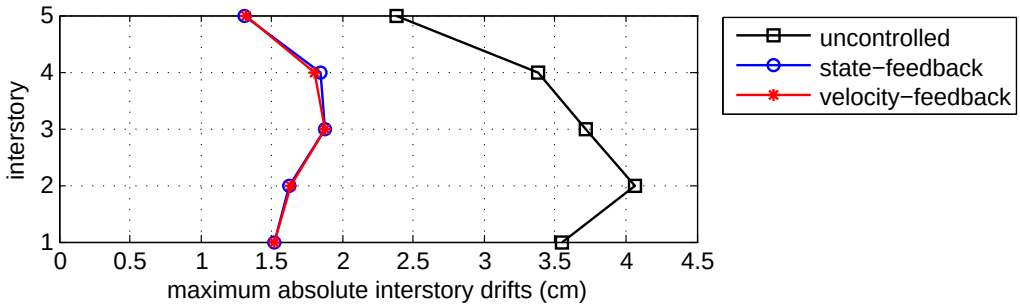

Figure 3: Maximum absolute interstory drift values: uncontrolled response (black line with squares), controlled response corresponding to the state-feedback controller (blue line with circles), and controlled response corresponding to the velocity-feedback controller (red line with asterisks).

The percentages of reduction in the maximum absolute interstory drifts obtained by the controlled configurations with respect to the uncontrolled response are presented in Table 1. The data in the table show that both controlled configurations provide percentages of reduction in the range 44%–60%, and that very similar results are obtained by the state-feedback controller and

Stories	0-1	1-2	2-3	3-4	4-5
State-feedback controller	57.04	59.96	49.48	45.31	45.00
Velocity-feedback controller	57.29	59.67	49.33	46.78	44.52

Table 1: Percentages of reduction in maximum absolute interstory drifts obtained by the state-feedback and velocity-feedback controllers with respect to the uncontrolled response.

the velocity-feedback controller. The maximum absolute control efforts $\hat{u}_i$ are collected in Table 2, and graphically displayed in Fig. 4. Here, we can see that practically the same maximum control efforts are required by the controlled configurations.

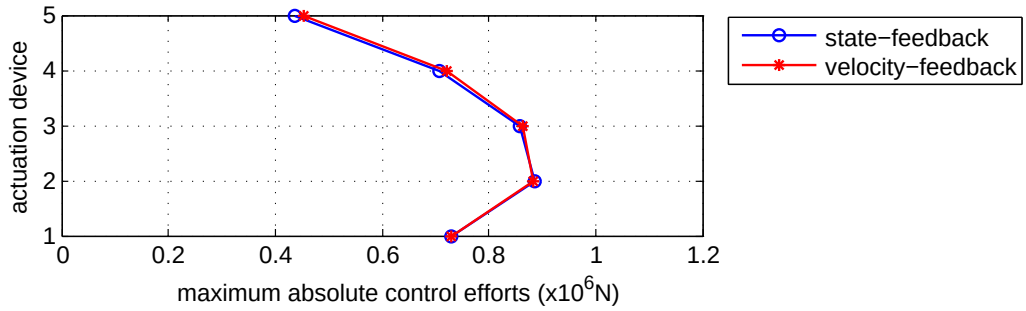

Figure 4: Maximum absolute control efforts corresponding to the state-feedback controller (blue line with circles), and the velocity-feedback controller (red line with asterisks).

Actuation device	1	2	3	4	5
State-feedback controller	0.7302	0.8846	0.8575	0.7075	0.4370
Velocity-feedback controller	0.7315	0.8838	0.8637	0.7230	0.4532

Table 2: Maximum absolute control efforts ($\times 10^6$N) corresponding to the state-feedback and velocity-feedback controllers.

Looking at the graphics in Fig. 3, we can see that the uncontrolled configuration attains the largest interstory peak-value for $r_2(t)$. The data in Table 1 show that the controlled configurations also obtain the largest percentage of reduction for $r_2(t)$. To provide a more complete picture of the vibrational attenuation achieved by the velocity-feedback controller, the interstory drifts $r_2(t)$ obtained by the uncontrolled configuration (black line) and velocity-feedback controlled configuration (thicker red line) are presented in Fig. 5. It has to be highlighted that the graphic of $r_2(t)$ corresponding to the state-feedback controller has not been included in Fig. 5 because it virtually overlaps with the velocity-feedback graphic. To supply a clear comparison of the time responses produced by these controllers, we can compute the difference

$$d_2(t) = r_2^{(s)}(t) - r_2^{(v)}(t), \tag{54}$$

where $r_2^{(s)}(t)$ and $r_2^{(v)}(t)$ denote the values of the interstory drifts $r_2(t)$ obtained for the state-feedback and the velocity-feedback controller, respectively. The graphic of the difference $d_2(t)$ is displayed in Fig. 6, where it can be appreciated that this difference is uniformly inferior to 0.1cm throughout the whole seismic event.

Remark 8. To prevent numerical errors, a relative accuracy of 10^{-8} has been set in the options of the MATLAB function `mincx()` when solving the LMI optimization problems P_s' and P_c' given in Eqs. (42) and (50), respectively.

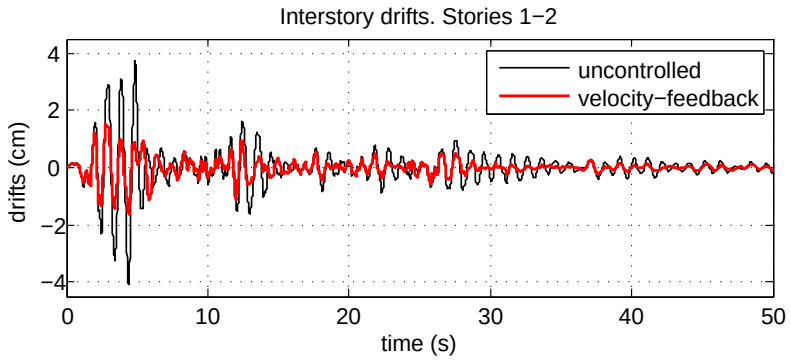

Figure 5: Interstory drifts for the stories 1–2. Vibrational response corresponding to the uncontrolled building and the velocity-feedback controlled configuration.

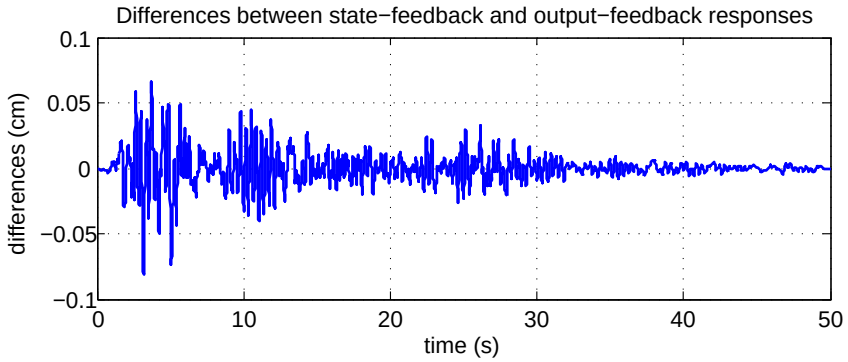

Figure 6: Differences in the interstory drifts obtained by the state-feedback controller and the output-feedback controller for the stories 1–2.

5. Conclusions and future directions

In this paper, an effective two-step procedure to design static output-feedback controllers has been presented. The proposed design methodology can be applied to any control problem that admits a state-feedback LMI formulation. In the first step, a state-feedback controller is computed. Next, the static output-feedback controller can be obtained by solving a single LMI optimization

problem, which can be easily derived from the state-feedback LMI formulation. To demonstrate the effectiveness of the proposed methodology, a static velocity-feedback H_∞ controller for the seismic protection of a five-story building has been designed with excellent results.

The new approach is based on recent results presented in [24], and provides a suitable solution to the feasibility issues encountered in [20–22]. After having successfully removed this important limitation, further research effort should be addressed to explore the potential of the proposed design methodology in more complex control problems, such as networked control [27, 28], switching systems [29, 30], robust control [31–33], fuzzy systems [34], or simultaneous stabilization [35].

Acknowledgments

This work was partially supported by the Spanish Ministry of Economy and Competitiveness through the grant DPI2012-32375/FEDER, and by the Norwegian Center of Offshore Wind Energy (NORCOWE) under grant 193821/S60 from the Research Council of Norway (RCN). NORCOWE is a consortium with partners from industry and science, hosted by Christian Michelsen Research.

References

[1] V. Syrmos, C. Abdallah, P. Dorato, K. Grigoriadis, Static output feedback – A survey, Automatica 33 (1997) 125–137.

[2] Z. Shu, J. Lam, An augmented system approach to static output-feedback stabilization with H_∞ performance for continuous-time plants, International Journal of Robust and Nonlinear Control 19 (2009) 768–785.

[3] R. Toscano, A simple method to find a robust output feedback controller by random search approach, ISA Transactions 45 (2006) 35–44.

[4] D. Moerder, A. Calise, Convergence of a numerical algorithm for calculating optimal output feedback gains, IEEE Transactions on Automatic Control 30 (1985) 900–903.

[5] Y.-Y. Cao, J. Lam, Y.-X. Sun, Static output feedback stabilization: an ILMI approach, Automatica 34 (1998) 1641–1645.

[6] J. Gadewadikar, F. Lewis, L. Xie, V. Kucera, M. Abu-Khalaf, Parameterization of all stabilizing H_∞ static state-feedback gains: application to output-feedback design, Automatica 43 (2007) 1597–1604.

[7] C. Crusius, A. Trofino, Sufficient LMI conditions for output feedback control problems, IEEE Transactions on Automatic Control 44 (1999) 1053–1057.

[8] E. Prempain, I. Postlethwaite, Static output feedback stabilisation with H_∞ performance for a class of plants, Systems and Control Letters 43 (2001) 159–166.

[9] G. Bara, M. Boutayeb, Static output feedback stabilization with H_∞ performance for linear discrete-time systems, IEEE Transactions on Automatic Control 50 (2005) 250–254.

[10] G. Bara, M. Boutayeb, A new sufficient condition for the static output feedback stabilization of linear discrete-time systems, in: Proceedings of the 45th IEEE Conference on Decision and Control, San Diego, California, USA, pp. 4723–4728.

[11] B. Spencer, S. Nagarajaiah, State of the art of structural control, Journal of Structural Engineering 129 (2003) 845–856.

[12] H. Li, L. Huo, Advances in structural control in civil engineering in China, Mathematical Problems in Engineering (2010) 1–23.

[13] F. Palacios-Quiñonero, J. Rossell, H. Karimi, Semi-decentralized strategies in structural vibration control, Modeling, Identification and Control 32 (2011) 57–77.

[14] F. Palacios-Quiñonero, J. Rubió-Massegú, J. Rossell, H. Karimi, Discrete-time multioverlapping controller design for structural vibration control of tall buildings under seismic excitation, Mathematical Problems in Engineering 2012 (2012) 1–20.

[15] F. Palacios-Quiñonero, J. Rubió-Massegú, J. Rossell, H. Karimi, Semiactive-passive structural vibration control strategy for adjacent structures under seismic excitation, Journal of the Franklin Institute 349 (2012) 3003–3026.
[16] H. Karimi, F. Palacios-Quiñonero, J. Rossell, J. Rubió-Massegú, Sequential design of multioverlapping controllers for structural vibration control of tall buildings under seismic excitation, Proceedings of the Institution of Mechanical Engineers, Part I: Journal of Systems and Control Engineering 227 (2013) 176–183.
[17] A. Zečević, D. Šiljak, Design of robust static output feedback for large-scale systems, IEEE Transactions on Automatic Control 49 (2004) 2040–2044.
[18] A. Zečević, D. Šiljak, Control design with arbitrary information structure constraints, Automatica 44 (2008) 2642–2647.
[19] A. Zečević, D. Šiljak, Control of Complex Systems. Structural Constraints and Uncertainty, Springer, 2010.
[20] J. Rubió-Massegú, F. Palacios-Quiñonero, J. Rossell, Decentralized static output-feedback H_∞ controller design for buildings under seismic excitation, Earthquake Engineering and Structural Dynamics 41 (2012) 1199–1205.
[21] F. Palacios-Quiñonero, J. Rubió-Massegú, J. Rossell, H. Karimi, Discrete-time static output-feedback semi-decentralized H_∞ controller design: an application to structural vibration control, in: Proceedings of the 2012 American Control Conference, Montréal, Canada, pp. 6126–6131.
[22] F. Palacios-Quiñonero, J. Rubió-Massegú, J. Rossell, H. Karimi, Optimal passive-damping design using a decentralized velocity-feedback H_∞ approach, Modeling, Identification and Control 33 (2012) 87–97.
[23] G. Balas, R. Chiang, A. Packard, M. Safonov, MATLAB^{TM} Robust Control Toolbox^{TM} 3. User's Guide, Version 4.2, The MathsWorks, Inc., 3 Apple Hill Drive. Natick, MA 01760–20, USA, 2012.
[24] J. Rubió-Massegú, J. Rossell, H. Karimi, F. Palacios-Quiñonero, Static output-feedback control under information structure constraints, Automatica 49 (2013) 313–316.
[25] N. Kurata, T. Kobori, M. Takahashi, N. Niwa, H. Midorikawa, Actual seismic response controlled building with semi-active damper system, Earthquake Engineering and Structural Dynamics 28 (1999) 1427–1447.
[26] A. Chopra, Dynamics of Structures. Theory and Applications to Earthquake Engineering, Prentice Hall, Upper Saddle River, New Jersey, USA, 3rd edition, 2007.
[27] R. Yang, P. Shi, G.-P. Liu, H. Gao, Network-based feedback control for systems with mixed delays based on quantization and dropout compensation, Automatica 47 (2011) 2805–2809.
[28] D. Zhang, X. Wang, Static output feedback control of networked control systems with packet dropout, International Journal of Systems Science 43 (2012) 665–672.
[29] L. Hou, G. Zong, Y. Wu, Finite-time control for switched delay systems via dynamic output feedback, International Journal of Innovative Computing, Information and Control 8 (2012) 4901–4913.
[30] S. Attia, S. Shalhi, M. Ksouri, Static switched output feedback stabilisation for linear discrete-time switched systems, International Journal of Innovative Computing, Information and Control 8 (2012) 3203–3213.
[31] R. Toscano, P. Lyonnet, Robust static output feedback controller synthesis using Kharitonov's theorem and evolutionary algorithms, Information Sciences 180 (2010) 2023–2028.
[32] V. Vaselý, D. Rosinová, V. Kucera, Robust static output feedback controller LMI based design via elimination, Journal of the Franklin Institute 348 (2011) 2468–2479.
[33] J. Dong, G.-H. Yang, Robust static output feedback control synthesis for linear continuous systems with polytopic uncertainties, Automatica 49 (2013) 1821–1829.
[34] W.-H. Ho, S.-H. Chen, I.-T. Chen, J.-H. Chou, C.-C. Shu, Design of stable and quadratic-optimal static output feedback controllers for TS-fuzzy-model-based control systems: an integrative computational approach, International Journal of Innovative Computing, Information and Control 8 (2012) 403–418.
[35] H.-B. Shi, L. Qui, Static output feedback simultaneous stabilisation via coordinates transformations with free variables, IET Control Theory and Applications 3 (2009) 1051–1058.